

The comparative Micro-CT analysis on trabecular bone density between hydroxyapatite gypsum pugger scaffold application and bovine hydroxyapatite scaffold application

Amiyatun Naini
Department of Prosthodontics,
Faculty of Dentistry, Universitas Jember,
Jember – Indonesia

ABSTRACT

Background: Generally, after tooth extraction, trauma is caused by bone damage, which leads to a decreased bone density. Bone damage repair should be conducted using a bone graft containing hydroxyapatite (HA). HA can be synthesised from gypsum pugger powder, which is abundant and easy to obtain. Hydroxyapatite gypsum pugger (HAGP) was successful with 100% hydroxyapatite purity level. **Purpose:** To compare the ratio of trabecular bone density in Wistar rats between HAGP scaffold application and bovine hydroxyapatite (BHA) scaffold application. **Methods:** This study is a laboratory experiment using 6 treatment groups, namely K (-) polyethylene glycol (PEG) 7, K (-) PEG 28, HAGP + PEG 7, HAGP + PEG 28, BHA + PEG 7, and BHA + PEG 28. HAGP scaffold freeze-drying. The rats were anaesthetised intramuscularly, and their left mandibular incisor was removed. The scaffold was applied to the mouse socket, followed by tissue decapitation after 7 and 28 days. The examination was carried out with micro-computed tomography (Micro-CT). Next, statistical analysis using a one-way analysis of variance (ANOVA) test was conducted ($p < 0.05$). **Results:** The ANOVA test result showed a difference in bone density between the treatment and control groups on days 7 and 28. The Least Significant Difference (LSD) test result revealed that there was no significant difference between K (-) PEG 28 and HAGP + PEG 7 ($p = 0.133$). Nevertheless, there were significant differences between the other groups. **Conclusion:** Based on the Micro-CT analysis, the trabecular bone density in Wistar rats following HAGP scaffold application is higher than that of BHA scaffold application.

Keywords: bone graft; bovine hydroxyapatite; hydroxyapatite gypsum pugger; micro-computed tomography

Correspondence: Amiyatun Naini, Department of Prosthodontics, Faculty of Dentistry, Universitas Jember. Jl. Kalimantan 37, Jember 68121, Indonesia. Email: amiyatunnini.fkg@unej.ac.id

INTRODUCTION

Trabecular bone is a part of the bone that appears spongy and is found near the ends of all bones, as well as in the middle region of the vertebral bones. An example is the jawbone, where the bone is not solid but full of holes connected by thin rods. The shape and structure of the trabecular bones are optimally regulated to withstand the loads imposed by functional activities. In dentistry, trabecular bone density is crucial in the dental implant system. Usually, the percentage density of trabecular bone ranges from 0.2–0.8 g/cm³, while its porosity is 75–95%.¹ Extraction of numerous teeth will lead to bone damage

trauma, causing the bone density to decrease. Bone density has a high correlation with fracture risk.²

Cases of trabecular bone damage are generally caused by trauma, post-tooth extraction and bone resorption. Repair of severe bone damage cases can be performed with the help of bone fillers, whereas the most preferred bone filling material is hydroxyapatite (HA) since it has a chemical composition similar to human bones and teeth.³ In this study, the gypsum used as a base material was taken from the Gamping mountain in the Pugger subdistrict as it is abundant, easy to obtain, and inexpensive; its calcium content is higher than commercial gypsum.⁴ The gypsum pugger was then successfully synthesised into

hydroxyapatite. The hydroxyapatite gypsum puger (HAGP) powder was subsequently developed into an HAGP scaffold with a 100% purity level of hydroxyapatite. Based on x-ray diffraction (XRD) and scanning electron microscope (SEM) scaffold examinations, the hydroxyapatite obtained had significant quantities of scaffold pores similar to the bovine hydroxyapatite (BHA) scaffold, which was the gold standard.⁵

According to Naini et al.,⁶ at 10% concentration, an HA scaffold from puger gypsum material can increase the number of osteoblasts and the area of bone trabeculae detected by histopathology anatomy (HPA) examination. Osteoblasts as cells bone constituents are formed from osteoprogenitor mesenchymal stem cells (MSC).⁷ Osteoblast cells as bone matrix constituents can even improve bone physical properties.⁸ Physical properties of bones in the form of mechanical strength are influenced by trabecular bone density.⁹

Moreover, the volume of trabecular bone density can be measured using a 3-dimensional Micro-CT tool. This can also display good trabecular structures with extremely high resolution using x-rays. It then adequately correlates with the histology of bone morphology so that it can be used as a standard.¹⁰ This study hypothesised that the trabecular bone density in Wistar rats after HAGP scaffold application would be higher than that of the BHA scaffold application. The aim of this research is therefore to analyse trabecular bone density in Wistar rats following HAGP scaffold application and compare the findings to that of a BHA scaffold application.

MATERIALS AND METHODS

This study is a laboratory experiment with a post-test only control group design. It is approved with a research ethic number: 247/KKEPK.FKG/X/2016. There were six treatment groups in this study: (a) control group (K (-)) using polyethylene glycol (PEG) for 7 days; (b) control group (K (-)) using PEG for 28 days; (c) treatment group 1 using HAGP + PEG for 7 days; (d) treatment group 2 using HAGP + PEG for 28 days; (e) treatment group 3 using BHA + PEG for 7 days; and (f) treatment group 4 using BHA + PEG for 28 days. The replication of each group consisted of 4 samples. Since there were 6 groups, 24 rats were needed. The sample size was determined with the Lemeshow formula.⁶ Furthermore, to make the HAGP scaffold, 250 mg of HAGP powder was mixed into 300 mg of gelatin and 10 ml of distilled water until homogeneous. The homogeneous mixture was then placed into a mould and a freeze-drying process was carried out.⁵ The BHA scaffold was obtained from the Tissue Bank of Dr Soetomo General Hospital Surabaya.

There were several parameters for determining the Wistar rats used in this study: 12–14 weeks of age, male, 200–250g weight, had one-week adaptation before treatment and looked after for 35 days. Certain treatments were given

to these rats. First, they were anaesthetised intramuscularly at a dose of 20–40 mg/kg body weight.¹¹ Second, asepsis of the mandibular left incisor was created with povidone-iodine and then the mandibular left incisor was extracted. Third, a scaffold was applied to the socket of each rat and sutured with a specific sewing thread, DR. SELLA Silk Braided asp 3/0 75 cm. Fourth, the sewing thread was removed on the seventh day after the extraction. After 7 and 28 days, the rats were sacrificed using 5 ml of ether in cotton and placed in a closed glass box for 5 minutes. Afterwards, each rat's left lower jaw tissue was carefully cut from the anterior to the posterior and washed with Phosphate Buffer Saline (PBS). The tissue was eventually placed in a 10% neutral buffer formalin fixation solution for 24 hours before scanned with the Micro-CT device. All the treatments were conducted in the Biochemistry Laboratory of the Medical Faculty, Universitas Airlangga, Surabaya.

Subsequently, tissue scanning was conducted using a Micro-CT device (Bruker SkyScan 1173 High Energy Micro-CT, Kontich, Belgium) with CTVox software version 3.3.1 (64-bit) and CTAn version 1.20.8.0 (64-bit). The scanning stage generates a grey-scale projection image in 16-bit Tagged Image File Format (TIFF) format, having an index interval between 0–65,535. The separation of tissue structure will ultimately occur, producing a visual image in 3D space. The analysis of each sample was carried out by calculating the Mean of Grayscale Index and the average thickness of the trabecular (Trabecular Thickness).¹² The Micro-CT examination was conducted in the Micro-CT laboratory of the Faculty of Mathematics and Natural Sciences, Institute of Technology Bandung.

Afterwards, statistical analysis was performed using a data normality test, the Shapiro Wilk test and a homogeneity test, the Levene test. The results of both tests showed that the data were normally distributed and homogeneous. Hence, a one-way ANOVA parametric test was performed using the IBM Statistical Package for Social Science (SPSS) version 23 for Windows (Armonk, New York, USA). When the test results indicated a significant one, the LSD multiple comparison test was then conducted to determine which pair of groups were different. The results of the LSD multiple comparison test revealed that there was no significant difference between K (-) PEG 28 and HAGP + PEG 7 with a p-value of 0.133. However, there were significant differences between the other groups with an ANOVA significant level of < 0.05.

RESULTS

The results of the HAGP scaffold and BHA scaffold application analysis using Micro-CT are illustrated in Figure 1. The results of bone density analysis using the Micro-CT tool are shown in Figure 2 and Table 1.

Subsequently, the results of bone density data analysed with the Shapiro Wilk normality test showed a p-value of > 0.05, indicating that the data were normally distributed.

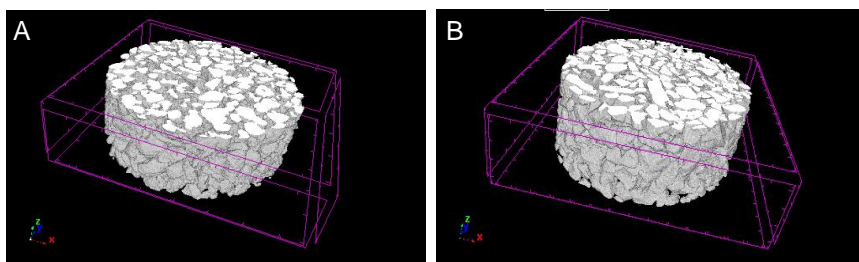


Figure 1. The morphology of the HAGP scaffold with an approximate size of 500 µm (A) and the morphology of the BHA scaffold with an approximate size of 250 µm (B).

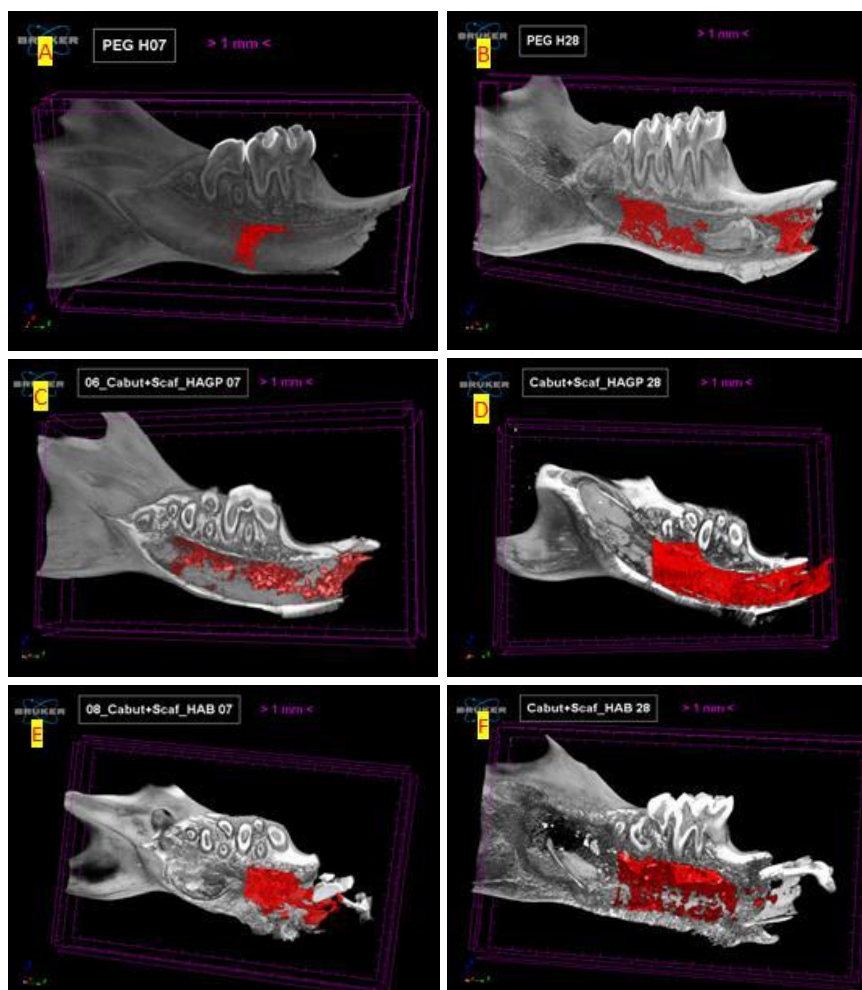


Figure 2. The results of bone density volume analysis are shown in red: (A) K (-) PEG 7, (B) K (-) PEG 28, (C) HAGP + PEG 7, (D) HAGP + PEG 28, (E) BHA + PEG 7, and (F) BHA + PEG 28.

Table 1. Description of bone density volume

Groups	N	Bone density volume (mm ³)				ANOVA (p)
		Mean	SD	Minimum	Maximum	
K (-) PEG 7	4	0.2200	0.09557	0.0679	0.3721	0.000
K (-) PEG 28	4	3.1300*	0.14583	2.8980	3.3620	
HAGP+PEG 7	4	3.4400*	0.13589	3.2238	3.6562	
HAGP+PEG 28	4	14.9200	0.22891	14.5558	15.2842	
BHA+PEG 7	4	6.3900	0.55731	5.5032	7.2768	
BHA+PEG 28	4	9.0100	0.23209	8.6407	9.3793	

Significant at $\alpha = 0.05$; the same superscript (*) showed no differences between groups using LSD multiple comparisons.

Next, Levene homogeneity test was carried out and revealed a p-value of 0.180, denoting that the data variance between groups was homogeneous. Thus, the ANOVA test analysis was then conducted, which resulted in a p-value of 0.000. This indicates that there was a difference in bone density between the treatment and control groups on days 7 and 28. To find out which group pairs were different; the LSD multiple comparison test was then employed. It showed a p-value of 0.133 between K (-) PEG 28 and HAGP + PEG 7, implying that there was no significant difference. Comparatively, the LSD multiple comparison test result for the other groups were significantly different.

The bone density volume observed with Micro-CT can be seen in Figure 2. The images showing mostly red sections were obtained from the HAGP + PEG 28 group relative to the other groups. Correspondingly, the highest average volume of bone density up to 14.9200 mm³ was found in the HAGP + PEG 28 group, followed by the BHA + PEG 28, BHA + PEG 7, HAGP + PEG 7, K (-) PEG 28 and (-) PEG 7 groups.

DISCUSSION

Severe cases of bone damage can be rehabilitated with the aid of bone grafts to restore bone density and thickness. In this study, bone substitution material from HAGP and BHA scaffold was used as a comparison. The morphology of both HAGP and BHA scaffold sizes along with alveolar bone density was analysed using Micro-CT.¹³

The Micro-CT analysis results showed that the morphology of HAGP scaffold size was unequal with that of the BHA scaffold size. The HAGP scaffold was approximately 500 µm, while the BHA scaffold was approximately 250 µm. This may be due to particle diffusion during the scaffold manufacturing process. Particle diffusion causes the movement of particles in the crystal toward the surface, forming a dendrite. The particle diffusion would bring the material above the dendrite at a rate greater than the surrounding surface. This process results in different shapes, once freeze-drying is done. Next, different pores will form on the HAGP and BHA scaffolds. The larger pore shape will facilitate larger and faster tissue formation and scaffold bioresorption.¹⁴

Moreover, alveolar bone density was analysed using Micro-CT to obtain both quantitative data as presented in Table 1 and qualitative data as illustrated in red in Figure 2. The data were then statistically analysed. The data analysis findings revealed variations in alveolar bone density between the HAGP, BHA and control groups. On days 7 and 28, the HAGP group had a higher alveolar bone density than the BHA group. This may be due to the different particle composition and morphology of the two scaffolds. The composition of calcium in HAGP (82.2%) was greater than BHA (81.86%). According to Crosman, the level of calcium can affect the absorption of x-rays in the bones.¹⁵ If there is an increase in the volume of mineralised bone density,

it can increase bone calcium as well as the absorption of x-rays. Calcium ions can stimulate the expression of bone markers on osteoblast cells for bone regeneration.¹⁶ Thus, the accumulation of calcium in the HAGP scaffold can provide a favourable environment for alveolar bone density to form new bone tissue growth.⁶

Furthermore, the two research materials compared in this study contain HA. HA is an alloplastic material used as a bone graft substitution that is bioactive and osteoconductive. HA in the form of particles can even have a regenerating effect on alveolar bone defects. HA is also known to have high crystallisation due to the sintering process and larger particle size than bone apatite.¹⁷ A porous HA scaffold can trigger good bone regeneration *in vivo*; the formation has a porosity size and three-dimensional shape that has the potential to be osteoconductive and osteogenic in the tooth socket.¹⁸

In Naini et al.'s⁵ previous research, based on a degradation test, the release of calcium and phosphate ions in the HAGP scaffold at the beginning of immersion was higher than in the BHA scaffold, resulting in a molecular chain-breaking process.¹⁹ The initial stage of biodegradation can raise the ion concentration in the bone defect, increasing bone growth/bone regeneration.²⁰ If there is rapid degradation, osteoblasts can be easily absorbed to accelerate the healing of the defect.^{21,22} Naini et al.⁶ stated that HAGP scaffold can increase osteoblasts and decrease osteoclasts during tooth socket healing with Hematoxylin Eosine (HE) examination. Osteoblast activity is higher in bone-forming parts than in bone-absorbing osteoclasts; connectivity is established and bone density increases, leading to a new bone growth process.²³ Micro-CT analysis is typically used to determine bone mass and microstructure that can be used in the study of bone metabolism in mice. Bone formation and mineralisation would then affect bone strength and mechanical stability, depending on the number and density of bones.

The novelty of this study is to compare trabecular bone density in Wistar rats using the HAGP scaffold application with that of the BHA scaffold application. It can be concluded that the trabecular bone density in Wistar rats is higher after the application of the HAGP scaffold than after the application of the BHA scaffold. Bone density analysis was conducted with Micro-CT tools. To develop better research on analysing trabecular bone density, it is suggested that further study should be performed using the same scaffold particle size with other parameters.

REFERENCES

1. Lita YA, Azhari A, Firman RN, Epsilawati L, Pramanik F. Aspek radiografis dan biologis tulang dalam penilaian kualitas tulang pada osteoporosis. *J Radiol Dentomaksilofasial Indones*. 2019; 3(2): 47–9.
2. Meyers MA, Chen PY, Lopez MI, Seki Y, Lin AYM. Biological materials: A materials science approach. *J Mech Behav Biomed Mater*. 2011; 4(5): 626–57.

3. Sadat-Shojai M, Khorasani MT, Dinpanah-Khoshdargi E, Jamshidi A. Synthesis methods for nanosized hydroxyapatite with diverse structures. *Acta Biomater*. 2013; 9(8): 7591–621.
4. Naini A, Rachmawati D. Composition analysis of calcium and sulfur on gypsum at the Puger District Jember Regency as an alternative gypsum dental material. *Dentika Dent J*. 2010; 15(2): 179–83.
5. Naini A, Sudiana IK, Rubianto M, Ferdiansyah, Mufti N. Characterization and degradation of hydroxyapatite gypsum puger (HAGP) freeze dried scaffold as a graft material for preservation of the alveolar bone socket. *J Int Dent Med Res*. 2018; 11(2): 532–6.
6. Naini A, Sudiana IK, Rubianto M, Kresnoadi U, Latief FDE. Effects of hydroxyapatite gypsum puger scaffold applied to rat alveolar bone sockets on osteoclasts, osteoblasts and the trabecular bone area. *Dent J (Majalah Kedokt Gigi)*. 2019; 52(1): 13–7.
7. Veni MAC, Rajathi P. Interaction between bone cells in bone remodelling. *J Acad Dent Educ*. 2: 1–6.
8. Sims NA, Martin TJ. Coupling signals between the osteoclast and osteoblast: How are messages transmitted between these temporary visitors to the bone surface? *Front Endocrinol (Lausanne)*. 2015; 6: 1–5.
9. Feng X, McDonald JM. Disorders of bone remodeling. *Annu Rev Pathol Mech Dis*. 2011; 6: 121–45.
10. Azhari A, Suprijanto S, Prafiadi H, Juliastuti E. Analisis kemampuan citra radiografi panoramik dalam mendeteksi kerapatan trabekula tulang dengan Micro CT sebagai baku standard -- Image analysis capability of detectinc panoramic radiographic trabecular bone density as standard with standard Micro CT. *Indones J Appl Sci*. 2014; 4(1): 1–5.
11. Kusumawati D. Bersahabat dengan hewan coba. Yogyakarta: Gadjah Mada University Press; 2004. p. 5–22.
12. Latief FDE, Sari DS, Fitri LA. Applications of Micro-CT scanning in medicine and dentistry: Microstructural analyses of a Wistar Rat mandible and a urinary tract stone. *J Phys Conf Ser*. 2017; 884: 012042.
13. Rochmatulloh AK, Fawziah UZ, Sumaryono RF, Feranie S, Latief FDE. Analisis citra digital untuk sampel batuan menggunakan Micro-CT Scanner Skyscan 1173. In: *Prosiding Seminar Nasional Fisika (E-Journal) SNF2017 UNJ*. Pendidikan Fisika dan Fisika FMIPA UNJ; 2017. p. 81–8.
14. Moisenovich MM, Arkhipova AY, Orlova AA, Drutskaya MS, Volkova S V, Zacharov SE, Agapov II, Kirpichnikov MP. Composite scaffolds containing silk fibroin, gelatin, and hydroxyapatite for bone tissue regeneration and 3D cell culturing. *Acta Naturae*. 2014; 6(1): 96–101.
15. Cosman F, de Beur SJ, LeBoff MS, Lewiecki EM, Tanner B, Randall S, Lindsay R, National Osteoporosis Foundation. Clinician's guide to prevention and treatment of osteoporosis. *Osteoporos Int*. 2014; 25(10): 2359–81.
16. Lü L-X, Zhang X-F, Wang Y-Y, Ortiz L, Mao X, Jiang Z-L, Xiao Z-D, Huang N-P. Effects of hydroxyapatite-containing composite nanofibers on osteogenesis of mesenchymal stem cells in vitro and bone regeneration in vivo. *ACS Appl Mater Interfaces*. 2013; 5(2): 319–30.
17. Jang SJ, Kim SE, Han TS, Son JS, Kang SS, Choi SH. Bone regeneration of hydroxyapatite with granular form or porous scaffold in canine alveolar sockets. *In Vivo*. 2017; 31(3): 335–41.
18. Kim JM, Son JS, Kang SS, Kim G, Choi SH. Bone regeneration of hydroxyapatite/alumina bilayered scaffold with 3 mm passage-like medullary canal in canine tibia model. *Biomed Res Int*. 2015; 2015: 1–6.
19. da Silva HM, de Lima IR, Bezerra PGP, Peregrino G, de Almeida Soares GD. In vitro dynamic degradation of strontium-hydroxyapatite granules. *Key Eng Mater*. 2011; 493–494: 205–8.
20. Sumathi S, Gopal B. In vitro degradation of multisubstituted hydroxyapatite and fluorapatite in the physiological condition. *J Cryst Growth*. 2015; 422: 36–43.
21. Wang Y, Yang X, Gu Z, Qin H, Li L, Liu J, Yu X. In vitro study on the degradation of lithium-doped hydroxyapatite for bone tissue engineering scaffold. *Mater Sci Eng C*. 2016; 66: 185–92.
22. Lin WC, Chuang CC, Yao C, Tang CM. Effect of cobalt precursors on cobalt-hydroxyapatite used in bone regeneration and MRI. *J Dent Res*. 2020; 99(3): 277–84.
23. Tanaka H, Mine T, Ogasa H, Taguchi T, Liang CT. Expression of RANKL/OPG during bone remodeling in vivo. *Biochem Biophys Res Commun*. 2011; 411(4): 690–4.